Time-Domain Analysis Approaches of Soil-Structure Interaction: A Comparative Study

Abdelrahman Taha, Niloofar Malekghaini, Hamed Ebrahimian, Ramin Motamed

Open Science Index, Structural and Construction Engineering Vol:16, No:12, 2022 publications.waset.org/10012867.pdf

***Abstract*—**This paper compares the substructure and direct approaches for soil-structure interaction (SSI) analysis in the time domain. In the substructure approach, the soil domain is replaced by a set of springs and dashpots, also referred to as the impedance function, derived through the study of the behavior of a massless rigid foundation. The impedance function is inherently frequency dependent, i.e., it varies as a function of the frequency content of the structural response. To use the frequency-dependent impedance function for time-domain SSI analysis, the impedance function is approximated at the fundamental frequency of the coupled soil-structure system. To explore the potential limitations of the substructure modeling process, a two-dimensional (2D) reinforced concrete frame structure is modeled and analyzed using the direct and substructure approaches. The results show discrepancy between the simulated responses of the direct and substructure models. It is concluded that the main source of discrepancy is likely attributed to the way the impedance functions are calculated, i.e., assuming a massless rigid foundation without considering the presence of the superstructure. Hence, a refined impedance function, considering the presence of the superstructure, shall alternatively be developed. This refined impedance function is expected to improve the simulation accuracy of the substructure approach.

***Keywords*—**Direct approach, impedance function, massless rigid foundation, soil-structure interaction, substructure approach.

I. Introduction

SEISMIC response of building structures is usually affected by the interaction between the structure and the supporting soil medium. SSI can be classified into two categories: kinematic and inertial interaction [1], [2]. Kinematic interaction is due to the presence of a surface or embedded foundation that is too stiff to follow the free-field deformation pattern. This results in the foundation experiencing a deformation pattern different from the free-field motion (FFM), often referred to as the foundation input motion (FIM). Inertial interaction is the result of transmitting inertial forces from the superstructure to the underlying complaint soil, which causes foundation movement that would not occur in a fixed-base structure. The resulting soil deformation is a source of flexibility and energy dissipation in the coupled soil-structure system [3]. Two energy dissipation mechanisms can result from the inertial SSI: hysteretic damping and radiation damping. The first mechanism is due to the nonlinear soil behavior, whereas the second is caused by the radiation of seismic waves from the structural base back into the soil domain. While the first mechanism is frequency independent, the second one is frequency dependent, i.e., it depends on the frequency content of the input motion and the dynamic characteristics of the superstructure.

Two common approaches exist to perform time-domain SSI analysis: direct approach and substructure approach [3]. In the direct approach, the surrounding and underlying soil and the superstructure are modeled in the same domain and are subjected to base excitations [2]. Due to its complexity and computational demand, this approach is limited to research and critical design applications. In the substructure approach, the soil domain is replaced by a set of springs and dashpots, referred to as the impedance function, reflecting the soil flexibility and damping, respectively. The substructure method is preferred and widely adopted in practice due to its simplicity and computational efficiency.

While both kinematic and inertial interactions are explicitly simulated in the direct SSI analysis approach, only the inertial interaction is accounted for in the substructure approach, through the introduction of the impedance function. To account for kinematic interaction effects in the substructure approach, the FIM is calculated and applied at the base of the substructure model (i.e., superstructure supported on the soil springs and dashpots). To calculate the FIM, analytical models can be used to relate FIM and FFM in the frequency domain – e.g., [4]. Alternatively, and more accurately, the FIM can be calculated by carrying out site response analysis (SRA) in the presence of a massless foundation. The ground motion at the foundation-soil interface will be the FIM [1].

The impedance function represents the force-deformation relationship at the foundation-soil interface in the frequency domain. Common impedance functions are developed by studying the behavior the soil-foundation system using analytical or numerical methods [5], [6]. This approach is based on the assumption that the soil-structure system can be divided into two subsystems: the soil-foundation and the superstructure, and that the responses of the two subsystems are uncoupled. Hence, the impedance function can be developed by studying the soil-foundation subsystem behavior. Then, the soil-foundation subsystem is to be replaced by the impedance function in the substructure model. Fig. 1 shows schematics of a 2D rigid foundation bonded an elastic half-space with three degrees of freedom: Δ_x, Δ_z, and $\emptyset$ denoting the foundation's horizontal displacement, vertical displacement, and rotation, respectively. R_x, R_z, and M are the corresponding applied forces, and b is the foundation half-length.

Abdelrahman Taha, Niloofar Malekghaini, Asst. Prof. Dr. Hamed Ebrahimian, and Assoc. Prof. Dr. Ramin Motamed are with the University of Nevada, Reno, NV 89557 USA (e-mail: abdelrahman.taha@nevada.unr.edu, nmalekghaini@nevada.unr.edu, hebrahimian@unr.edu, motamed@unr.edu).

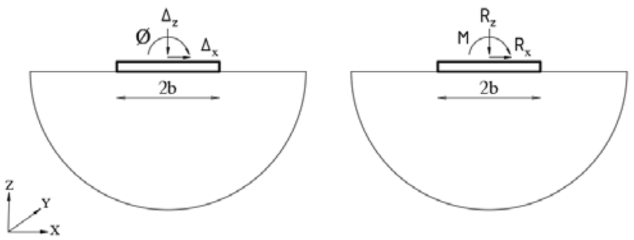

Fig. 1 Schematic presentation of a 2D rigid strip footing resting on an elastic half-space

The soil dynamic stiffness matrix – i.e., impedance function – relates the displacement to force vector as follows [5]:

$$\begin{Bmatrix} R_z \\ R_x \\ M/b \end{Bmatrix} = \pi\mu \begin{bmatrix} K_z + i\omega C_z & 0 & 0 \\ 0 & K_x + i\omega C_x & K_{xy} + i\omega C_{xy} \\ 0 & K_{yx} + i\omega C_{yx} & K_{yy} + i\omega C_{yy} \end{bmatrix} \begin{bmatrix} \Delta_z \\ \Delta_x \\ \emptyset/b \end{bmatrix} \quad (1)$$

in which the terms K_x, K_{xy}, K_{yx}, and K_{yy} are the dimensionless stiffnesses, C_x, C_{xy}, C_{yx}, and C_{yy} are the dimensionless damping coefficients, and μ is the soil shear modulus. The coupling terms K_{xy}, K_{yx}, C_{xy}, *and* C_{yx} are equal, and the dynamic stiffness matrix is symmetric. To use the frequency-dependent impedance function for time-domain SSI analysis, a simplified approach is introduced in [3]. In this approach, the impedance function is evaluated at a single frequency corresponding to the fundamental frequency of the soil-structure system.

In this paper, we explore the potential limitations of the substructure approach by means of numerical analysis of a case study. Section II explains the modeling details of the case study. The analysis results are presented in Section III. Further justification and interpretation of the analysis results are pursued in Section IV. Finally, the main conclusions and recommendations of the paper are summarized in Section V.

II. Cast Study

This study is focused on evaluating the response of 2D linear structural systems with rigid foundation resting on linear elastic half-space in plain-strain setting and subjected to vertically propagating shear waves (SV-waves). In this section, the design and modeling details of a case study frame structure are explained for both the direct and substructure approaches. The finite element analysis framework OpenSees [7] is used for the modeling and response simulation.

In this case study, the structural and soil properties are selected to result in significant inertial SSI. In their work, Stewart et al. [8] showed that the most important parameter controlling inertial interaction is the structure-to-soil stiffness ratio ($^{h}/_{V_sT}$), where h is the building height, V_s is the soil shear wave velocity, and T is the fixed-base building period. It was shown that inertial interaction is negligible if this ratio is less than 0.1, whereas it becomes more significant for values more than 0.1. More specifically, this ratio was found to be less than 0.1 for moment frame structures and between 0.1 and 0.5 for shear wall and braced frame structures [3].

The studied building herein is an eight-story, two-bay, reinforced concrete (RC) frame structure with story height of 3 m, bay length of 5 m, and foundation length of 12 m. The column and beam cross-sectional dimensions are 50 cm × 90 cm and 30 cm × 60 cm, respectively. The concrete modulus of elasticity is assumed to be 30 GPa. The structural mass is 100 ton per floor. The fixed-base building period is 1.0 s. The soil domain is assumed to have a shear wave velocity of 100 $^{\mathrm{m}}/_{\mathrm{s}}$ and a Poisson's ratio of 0.25. The soil density is equal to 1.7 $^{\mathrm{ton}}/_{\mathrm{m}^3}$. Given the system properties, the ratio $^{h}/_{V_sT}$ is found to be equal to 0.24. Hence, significant inertial SSI effects are expected. No damping is considered for either the structure or the soil domain; hence, the only source of energy dissipation in the system is radiation damping.

The direct model is developed by explicitly modeling both the structural system and the supporting soil medium as shown in Fig. 2. The response simulation of such large models is typically computationally expensive. To reduce the computational cost, the parallel analysis capabilities in OpenSees are utilized. For this purpose, the OpenSeesMP application is employed, which requires manual decomposition of the domain [7]. Fig. 2 shows schematically the direct model division into 10 parts. The frame elements are modeled using *elasticBeamColumn* elements. The foundation is also modeled using *elasticBeamColumn* with large cross-sectional dimensions to satisfy the rigid foundation assumption. The soil domain is modeled using four-noded *quad* elements with plane-strain formulation. The thickness of the quad elements is 1 m; the in-plane element size is 1 m × 1 m to ensure that the ratio between the element size and the minimum wavelength of the waves propagating in the soil domain is less than 1/12 [9]. The soil domain's depth and width are 50 m and 100 m, respectively. Perfect bond between the foundation and soil surface is enforced using the *EqualDOF* constraints. To simulate a semi-infinite soil medium using a finite soil domain, the outgoing waves at the model boundaries should not reflect back into the soil domain. For this purpose, the free-field tractions are defined on the soil domain boundaries using the boundary elements developed by Nielsen [10].

The substructure model is created by replacing the soil domain using the impedance function developed by Luco and Westmann [5]. This function was developed for a rigid strip footing bonded to an elastic half-space, which is similar to this case study. Since the structure here has a surface foundation and is subjected to SV-waves, the vertical impedance terms (K_z and C_z) are neglected and replaced by a roller support as shown in Fig. 3. Moreover, the coupling terms (K_{xy}, K_{yx}, C_{xy}, and C_{yx}) are neglected since their effects are relatively small and insignificant for surface foundation [11]. The springs and dashpots are attached to the centroid of the foundation as shown in Fig. 3.

The evaluation of the impedance function requires calculating the flexible-base fundamental frequency. To calculate this frequency, the structural base in the direct model is subjected to a unit impulse, and the roof acceleration response is recorded. This represents the impulse response function (IRF) for the coupled system, which is used to find the fundamental frequency. The fundamental frequency of the system is found

Open Science Index, Structural and Construction Engineering Vol:16, No:12, 2022 publications.waset.org/10012867.pdf

to be equal to 0.35 Hz through calculation of the Fourier transform of the IRF. To evaluate the impedance function, the dimensionless frequency parameter, i.e., $a_0 = {}^{\omega b}/_{V_s}$, has to be calculated first, where ω is the fundamental circular frequency. Given a frequency of 0.35 Hz, a_0 is equal to 0.13 (i.e., $a0 = (2\pi \times 0.35) \times {}^{6}/_{100} = 0.13$). The values of the dimensionless impedance parameters corresponding to $a_0 = 0.13$ are presented in Table I.

TABLE I
PARAMETERS OF THE IMPEDANCE FUNCTION

Parameter	K_x	K_{yy}	C_x	C_{yy}
Value	0.35	0.71	0.188	0.015

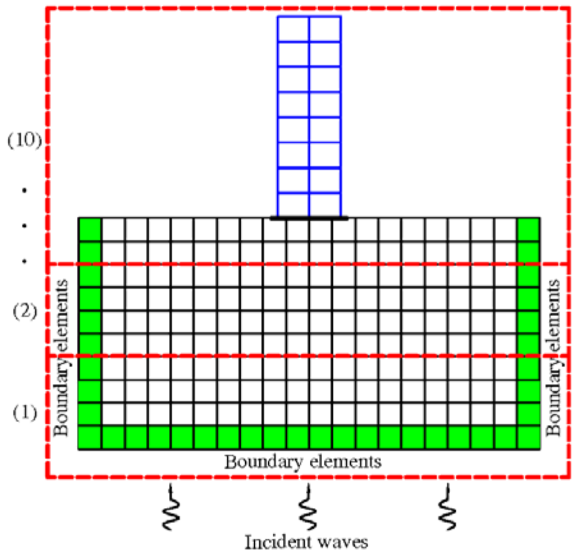

Fig. 2 Direct model: Schematic division of the model into 10 parts for parallel processing in OpenSeesMP

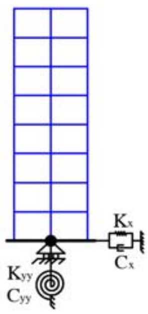

Fig. 3 Substructure model

III. ANALYSIS RESULTS

The case study structure is subjected to two input motions: seismic motion and harmonic motion. The 2007 Chuetsu-oki earthquake (Kashwazaki NPP station – NS component) is adopted for the seismic analysis, obtained from the NGA-west 2 ground motion database [12]. Fig. 4 (a) shows the acceleration time history of this earthquake, while Fig. 4 (b) shows the acceleration response spectrum of the FIM. The harmonic motion is defined as a sinusoidal function with the fundamental frequency of the coupled system (i.e., 0.35 Hz).

In the direct model, the velocity time history of the input motion is applied to the boundary elements of the bottom layer [7]. In the substructure model, the FIM is calculated using one-dimensional (1D) SRA. Since the incident waves are vertically propagating shear waves and the foundation is rested on the soil surface, there will be no kinematic interaction, and hence, the FIM is similar to the FFM calculated using 1D SRA [1].

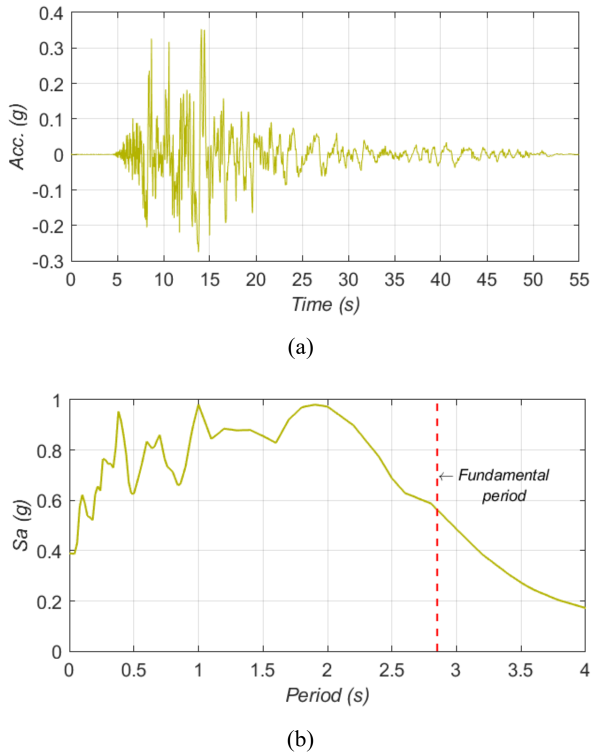

Fig. 4 2007 Chuetsu-oki earthquake: (a) Acceleration time history, and (b) Acceleration response spectrum (5% damping)

The dynamic time history analyses are performed using the time-stepping Newmark's constant average acceleration method [13]. The analysis time-step size is 0.01 s for both seismic and harmonic analyses to ensure adequate temporal discretization [14]. Fig. 5 shows the seismic absolute acceleration responses of the roof and fourth floor. As can be seen, the discrepancy between the two model responses is non-negligible. One potential reason for the observed discrepancy is the presence of higher-frequency responses in the direct model that cannot be reproduced in the substructure model, wherein the frequency-dependent impedance function is evaluated at a single frequency, i.e., the flexible-base fundamental frequency [15], [16]. However, a particularly significant mismatch between the frequency-domain responses around the fundamental frequency can be observed in Figs. 5 (b) and (d), which implies that the presence of higher-frequency responses is not the only and most effective source of discrepancy. To eliminate the effect of higher-frequency responses, the two models are subjected to a harmonic motion with the flexible-base fundamental frequency.

Fig. 6 presents the harmonic absolute acceleration responses

Open Science Index, Structural and Construction Engineering Vol:16, No:12, 2022 publications.waset.org/10012867.pdf

Open Science Index, Structural and Construction Engineering Vol:16, No:12, 2022 publications.waset.org/10012867.pdf

of the roof and fourth floor. Once more, a disparity between the two model responses can be noticed. These results confirm that the discrepancy is most significant around the flexible-base fundamental frequency. Hence, we argue that the main reason for this discrepancy is most likely that the soil-foundation subsystem behavior around the flexible-base fundamental frequency changes due to the presence of the superstructure. That is, the assumption of the uncoupled responses of the superstructure and the soil-foundation subsystems is likely inaccurate. This consequently may question the use of the soil-foundation impedance functions for the analysis of soil-structure systems. This difference is further explained in the next section.

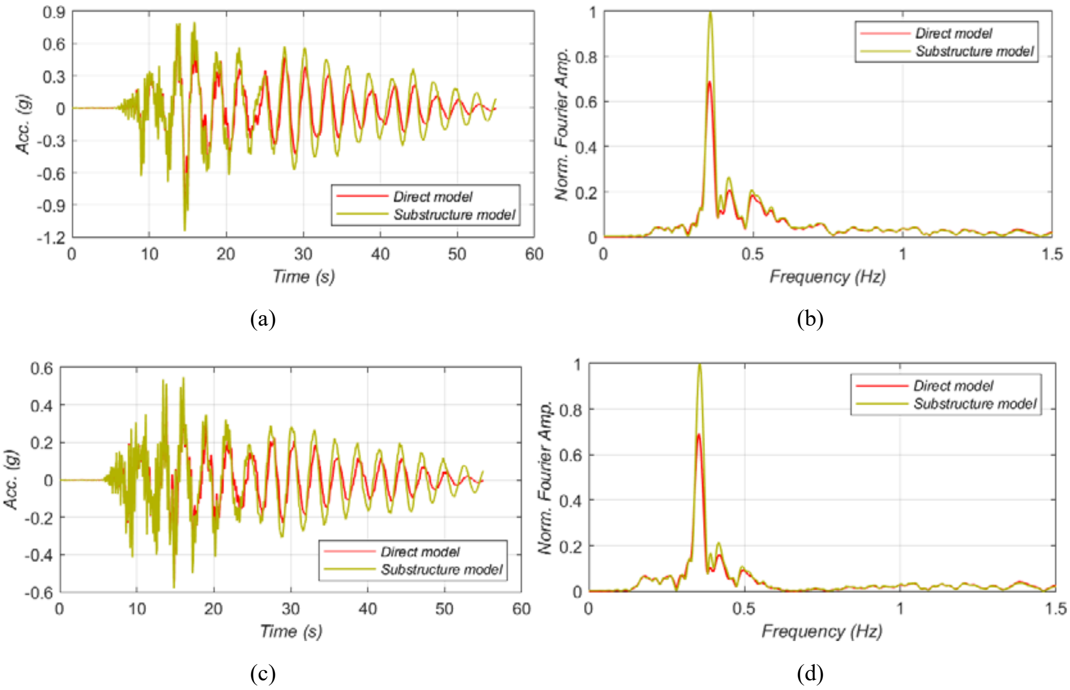

Fig. 5 Seismic absolute acceleration response, (a) Roof acceleration, (b) Fourier transform of the roof acceleration, (c) Fourth-floor acceleration, and (d) Fourier transform of the fourth-floor acceleration

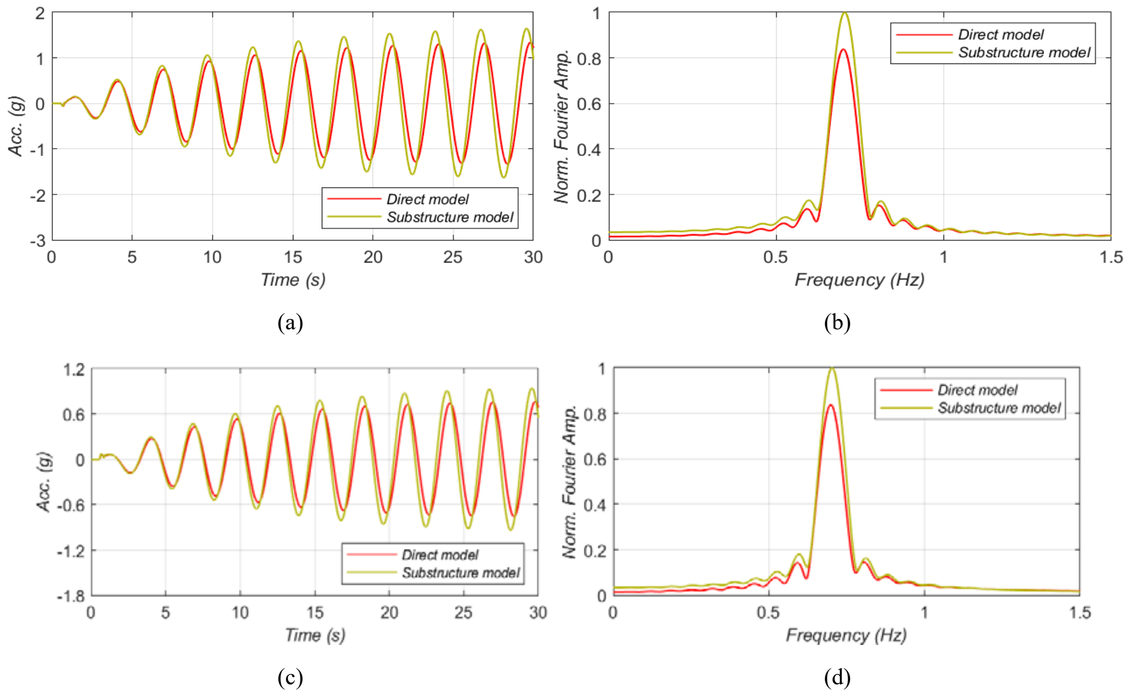

Fig. 6 Harmonic absolute acceleration response, (a) Roof acceleration, (b) Fourier transform of the roof acceleration (c) Fourth-floor acceleration, and (d) Fourier transform of the fourth-floor acceleration

Open Science Index, Structural and Construction Engineering Vol:16, No:12, 2022 publications.waset.org/10012867.pdf

IV. Discussion

In the previous section, we argued that the reason for the discrepancy between the fundamental-frequency responses of the substructure and direct models is likely due to developing the impedance function by studying the response of the soil-foundation subsystem. This can be explained by comparing the behavior of the soil-foundation subsystem and the soil-structure system around the flexible-base fundamental frequency. The fundamental mode of the soil-structure system is a coupled horizontal-rotational mode, unlike the soil-foundation subsystem, in which the foundation horizontal and rotational responses are uncoupled. This makes the soil deformation field and reflecting wavefield in the case of soil-foundation different from their counterparts in the case of soil-structure. Fig. 7 shows schematically the resulting soil deformation field and wavefield from incident SV-waves for both cases. In the soil-foundation case, the SV-waves incident on the foundation causes only horizontal deformation of the foundation (u_g) and then reflects back into the soil domain. On the other hand, the foundation in the presence of the superstructure, i.e., the soil-structure case, undergoes both horizontal displacement (u_g) and rotation (θ_g), which creates a reflecting wavefield comprising three types of waves: SV-waves, compressional (P-) waves, and Rayleigh (R-) waves.

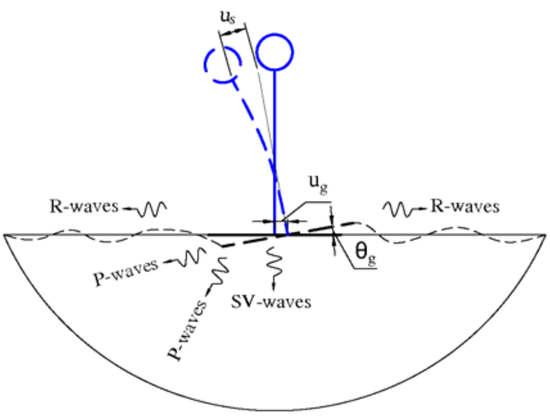

(a)

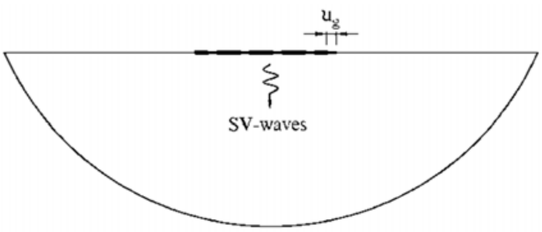

(b)

Fig. 7 Schematic representation of the soil deformation field and wavefield resulting from incident SV-waves, (a) Soil-structure, and (b) Soil-foundation

To show the wavefield of each case, we study the synthetic seismograms developed using the acceleration response. The surface R-waves can be captured through a seismogram along the soil surface, while showing the P-waves requires plotting a subsurface seismogram. To obtain a clear wavefield using synthetic seismograms, a larger soil domain is used with a 100 m depth and 500 m width. The subsurface seismogram is taken at 90 m depth below the surface. The elevation level of subsurface seismogram is relatively deep to avoid significant interference between the incident and reflecting waves at this level.

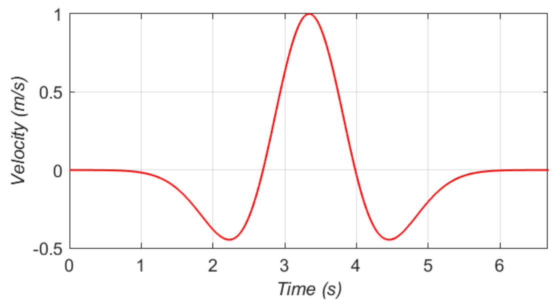

(a)

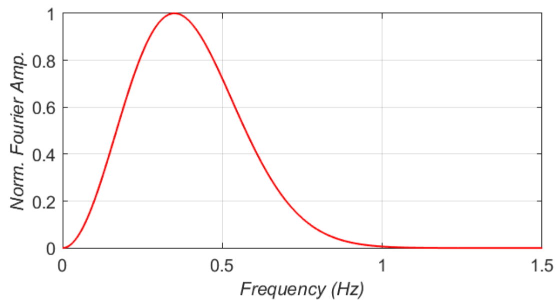

(b)

Fig. 8 Ricker pulse, (a) Velocity time history, and (b) Fourier transform of the velocity time history

A Ricker pulse signal is used as the input motion to the direct model, and its dominant frequency is chosen to be the fundamental frequency of the coupled system (i.e., 0.35 Hz). Fig. 8 shows the velocity time history of the Ricker pulse and its Fourier transform.

The surface horizontal and vertical synthetic seismograms are presented in Figs. 9 and 10. R-waves can be observed in Figs. 9 (a) and 10 (a) for the soil-structure system. The soil-foundation subsystem, on the other hand, translates horizontally without rotation; hence, it does not produce any R-waves or P-waves, as can be seen in Figs. 9 (b) and 10 (b). The subsurface seismograms for the soil-structure system are shown in Fig. 11. Both incident and reflecting SV-waves can be observed in the horizontal acceleration seismogram; the scattering P-waves can be detected in both acceleration seismograms.

The observed difference in the displacement field and wavefield of the soil-structure system and the soil-foundation subsystem is most likely the reason that the soil-foundation impedance function does not provide accurate results when incorporated in the substructure model. This is because the impedance function represents the flexibility and damping mechanisms (or the displacement field and radiating wavefield)

Open Science Index, Structural and Construction Engineering Vol:16, No:12, 2022 publications.waset.org/10012867.pdf

of the soil domain supporting the structure. Since the soil displacement field and wavefield produced in the soil-structure system is different from its soil-foundation counterpart, their respective impedance functions are expected to be different as well. Consequently, improving the simulation accuracy of the substructure approach requires developing a refined impedance function considering the presence of the superstructure.

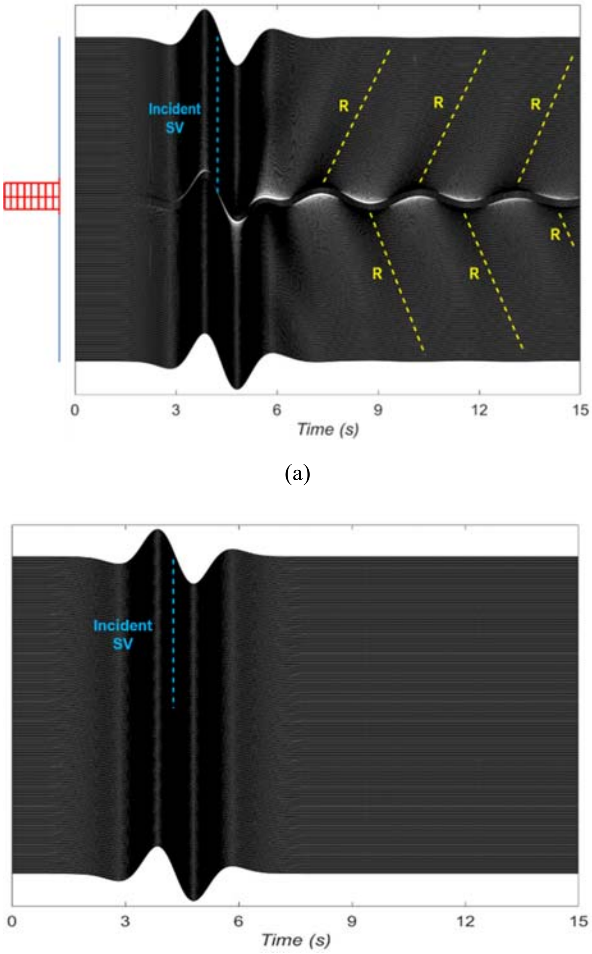

(a)

(b)

Fig. 9 Surface seismograms using horizontal acceleration, (a) Soil-structure, and (b) Soil-foundation

V. Conclusions

Accurate characterization of SSI is usually crucial for the seismic analysis and design of building structures. Since the substructure approach is the current state-of-practice of SSI analysis, we attempted to quantify the simulation accuracy and potential limitations of this approach as compared to the more accurate, computationally demanding direct approach.

For this purpose, a time-domain numerical study was conducted on a 2D RC frame structure rested on the surface of an elastic half-space, in which the system response was simulated using both the direct and substructure approaches. The soil-structure system was subjected to a seismic motion and a harmonic motion. The substructure approach was shown to provide inaccurate simulation of the system response under both motions. Expectedly, we observed a discrepancy between the higher-frequency responses, which is typically attributed to the common practice of evaluating the frequency-dependent impedance function at a single frequency (i.e., the flexible-base fundamental frequency). Furthermore, we observed a more significant discrepancy between the fundamental-frequency responses, and we hypothesized that it is likely due to developing the impedance function by studying the behavior of the soil-foundation subsystem. To examine this hypothesis, we studied the soil deformation fields and wavefields for the soil-structure system and the soil-foundation subsystem. The study showed considerable difference between the soil deformation fields and scattering wavefields of both systems. Since the impedance function represents soil flexibility (i.e., deformation field) and damping (i.e., radiating wavefield), the respective impedance functions of both systems are expected to be different.

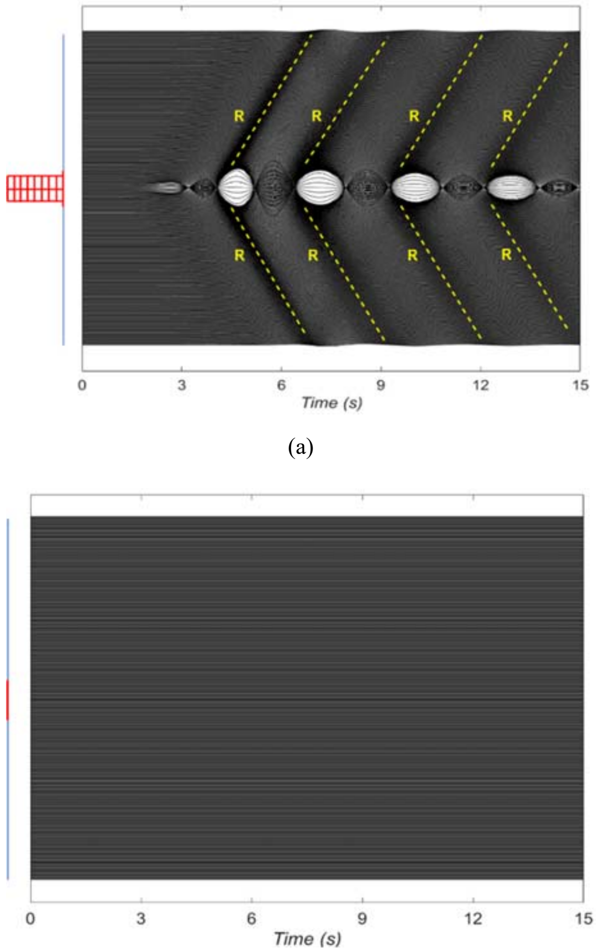

(a)

(b)

Fig. 10 Surface seismograms using vertical acceleration, (a) Soil-structure, and (b) Soil-foundation

Open Science Index, Structural and Construction Engineering Vol:16, No:12, 2022 publications.waset.org/10012867.pdf

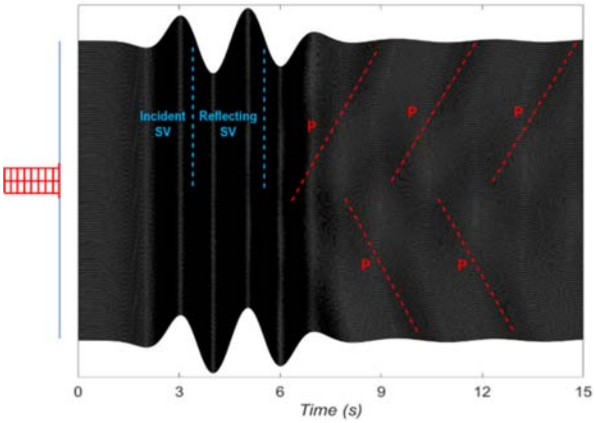

(a)

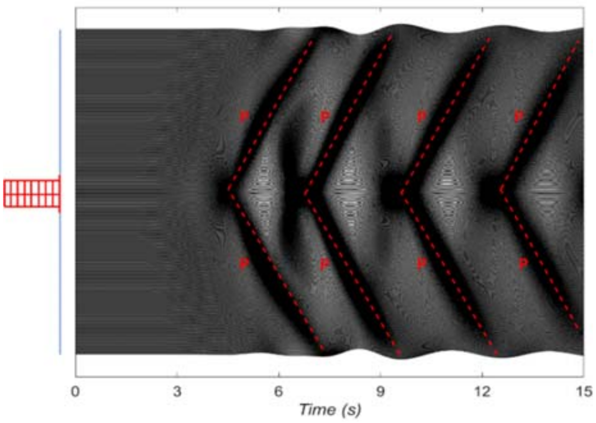

(b)

Fig. 11 Subsurface seismograms for the soil-structure system, (a) Using horizonal acceleration, and (b) Using vertical acceleration

The current study highlighted the limitations of the substructure approach; more specifically, the assumption of the uncoupling between the superstructure and the soil-foundation subsystem responses, and hence, developing the impedance function by studying the behavior of the soil-foundation subsystem was argued to be the key reason for discrepancy between the two SSI analysis approaches. Therefore, future studies on developing a refined impedance function considering the presence of the superstructure are suggested to improve the simulation accuracy of the substructure approach.

Acknowledgment

This material is based upon work supported by the U.S. Geological Survey under Grant No. (G20AP00115-01).

Disclaimer

The views and conclusions contained in this document are those of the authors and should not be interpreted as representing the opinions or policies of the U.S. Geological Survey. Mention of trade names or commercial products does not constitute their endorsement by the U.S. Geological Survey.

References

[1] S. L. Kramer, *Geotechnical earthquake engineering*. Pearson Education India, 1996.

[2] John P.Wolf, *Dynamic Soil-Structure Interaction. Prentice-Hall international series in civil engineering and engineering mechanics*. 1985.

[3] NIST, "NIST GCR 12-917-21 Soil-Structure Interaction for Building Structures," 2012.

[4] G. Mylonakis, S. Nikolaou, and G. Gazetas, "Footings under seismic loading: Analysis and design issues with emphasis on bridge foundations," *Soil Dyn. Earthq. Eng.*, vol. 26, no. 9, pp. 824–853, 2006.

[5] J. E. Luco and R. A. Westmann, "Dynamic response of a rigid footing bonded to an elastic half space," 1972.

[6] E. E. Seylabi, C. Jeong, and E. Taciroglu, "On numerical computation of impedance functions for rigid soil-structure interfaces embedded in heterogeneous half-spaces," *Comput. Geotech.*, vol. 72, pp. 15–27, 2016.

[7] F. McKenna, "OpenSees: a framework for earthquake engineering simulation," *Comput. Sci. Eng.*, vol. 13, no. 4, pp. 58–66, 2011.

[8] J. P. Stewart, G. L. Fenves, and R. B. Seed, "Seismic soil-structure interaction in buildings. I: Analytical methods," *J. Geotech. Geoenvironmental Eng.*, vol. 125, no. 1, pp. 26–37, 1999.

[9] J. Lysmer and R. L. Kuhlemeyer, "Finite dynamic model for infinite media," *J. Eng. Mech. Div.*, vol. 95, no. 4, pp. 859–877, 1969.

[10] A. H. Nielsen, "Absorbing boundary conditions for seismic analysis in ABAQUS," *ABAQUS users' Conf.*, pp. 359–376, 2006.

[11] A. Pais and E. Kausel, "Approximate formulas for dynamic stiffnesses of rigid foundations," *Soil Dyn. Earthq. Eng.*, vol. 7, no. 4, pp. 213–227, 1988, doi: 10.1016/S0267-7261(88)80005-8.

[12] T. Ancheta *et al.*, "PEER NGA-West2 database: A database of ground motions recorded in shallow crustal earthquakes in active tectonic regions," 2012.

[13] A. K. Chopra, *Dynamics of structures*. Pearson Education India, 2007.

[14] Y. Wang, V. Murti, and S. Valliappan, "Assessment of the accuracy of the Newmark method in transient analysis of wave propagation problems," *Earthq. Eng. Struct. Dyn.*, vol. 21, no. 11, pp. 987–1004, 1992.

[15] D. S. Kusanovic, E. Seylabi, and D. Asimaki, "Optimization of frequency domain impedances for time-domain response analyses of building structures with rigid shallow foundations," *Earthq. Spectra*, vol. 37, no. 3, pp. 1955–1979, 2021.

[16] D. Kusanovic, E. Seylabi, and D. Asimaki, "System identification of soil-structure interaction mechanisms for building structures," in *SMIP18 seminar on utilization of strong-motion data*, 2018, pp. 53–68.